

Supporting Information for

Architectures and DFT calculations of polyrotaxane MOFs with nanoscale macrocycles†

**Ming-Dao Zhang^{*,a,b} Bao-Hui Zheng,^c Liang Chen,^a Min-Dong Chen,^a Tao Tao,^{a,b} Kai Chen,^a
and Hui Cao^{*,a}**

^a*Jiangsu Key Laboratory of Atmospheric Environment Monitoring and Pollution Control, Jiangsu
Collaborative Innovation Center for Atmospheric Environment & equipment technology, School of
Environmental Science and Engineering, Nanjing University of Information Science & Technology,
Nanjing 210044, Jiangsu, P. R. China.*

^b*State Key Laboratory of Coordination Chemistry, Nanjing University, Nanjing 210093, P. R. China.*

^c*Institute of Chemical Materials, Chinese Academy of Engineering Physics, Mianyang 621999,
Sichuan, P. R. China. E-mail: zhengbaohui305@126.com.*

Table S1 Selected bond lengths (\AA) and angles ($^{\circ}$) by X-ray and theoretical calculations for complexes **1** and **2**

Bond lengths (\AA) for 1 ^a			
N(1)-Ni(1)	2.030(3)	Ni(1)-O(3)	2.213(2)
Ni(1)-N(2)#1	2.062(3)	Ni(1)-O(4)	2.063(2)
Ni(1)-O(1)	2.084(2)	Ni(1)-O(2)	2.143(2)
Bond lengths (\AA) for 2 ^b			
N(1)-Zn(1)	2.087(4)	Zn(1)-N(2)#1	2.051(4)
O(2)-Zn(1)	2.006(3)	O(4)-Zn(1)	1.956(3)
Bond angles ($^{\circ}$) for 1 ^a			
N(1)-Ni(1)-N(2)#1	96.00(10)	N(1)-Ni(1)-O(4)	100.65(10)
N(2)#1-Ni(1)-O(4)	95.22(9)	N(1)-Ni(1)-O(1)	162.35(10)
N(2)#1-Ni(1)-O(1)	89.76(10)	O(4)-Ni(1)-O(1)	95.40(8)
N(1)-Ni(1)-O(2)	100.19(10)	N(2)#1-Ni(1)-O(2)	98.13(10)
O(4)-Ni(1)-O(2)	153.84(8)	O(1)-Ni(1)-O(2)	62.40(8)
N(1)-Ni(1)-O(3)	93.23(9)	N(2)#1-Ni(1)-O(3)	156.21(9)
O(4)-Ni(1)-O(3)	61.46(8)	O(1)-Ni(1)-O(3)	87.99(9)
O(2)-Ni(1)-O(3)	101.75(8)		
Bond angles ($^{\circ}$) for 2 ^b			
O(4)-Zn(1)-O(2)	135.02(15)	O(4)-Zn(1)-N(2)#1	117.83(15)
O(2)-Zn(1)-N(2)#1	97.82(15)	O(4)-Zn(1)-N(1)	101.55(15)
O(2)-Zn(1)-N(1)	95.74(15)	N(2)#1-Zn(1)-N(1)	102.82(15)

^a Symmetry codes for **1**: #1 = $-x + 2, -y + 1, -z + 1$; ^b Symmetry codes for **2**: #1 = $x + 3, -y + 1, -z + 1$.

Table S2. Hydrogen-bonding geometry (\AA , $^\circ$) for complex **1**.

D-H \cdots A	d(H \cdots A)	d(D \cdots A)	\angle D-H \cdots A
O1W-H1WB \cdots O2	2.13	2.898(4)	150
O1W-H1WC \cdots O3	2.42	2.899(4)	115
O2W-H2WA \cdots O1W	2.33	2.775(5)	113
O2W-H2WB \cdots O1W	2.49	2.775(5)	101

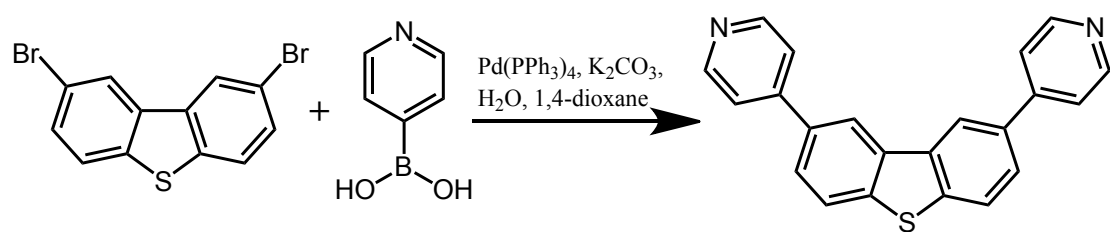


Fig. S1. Synthetic reaction of DPDBT

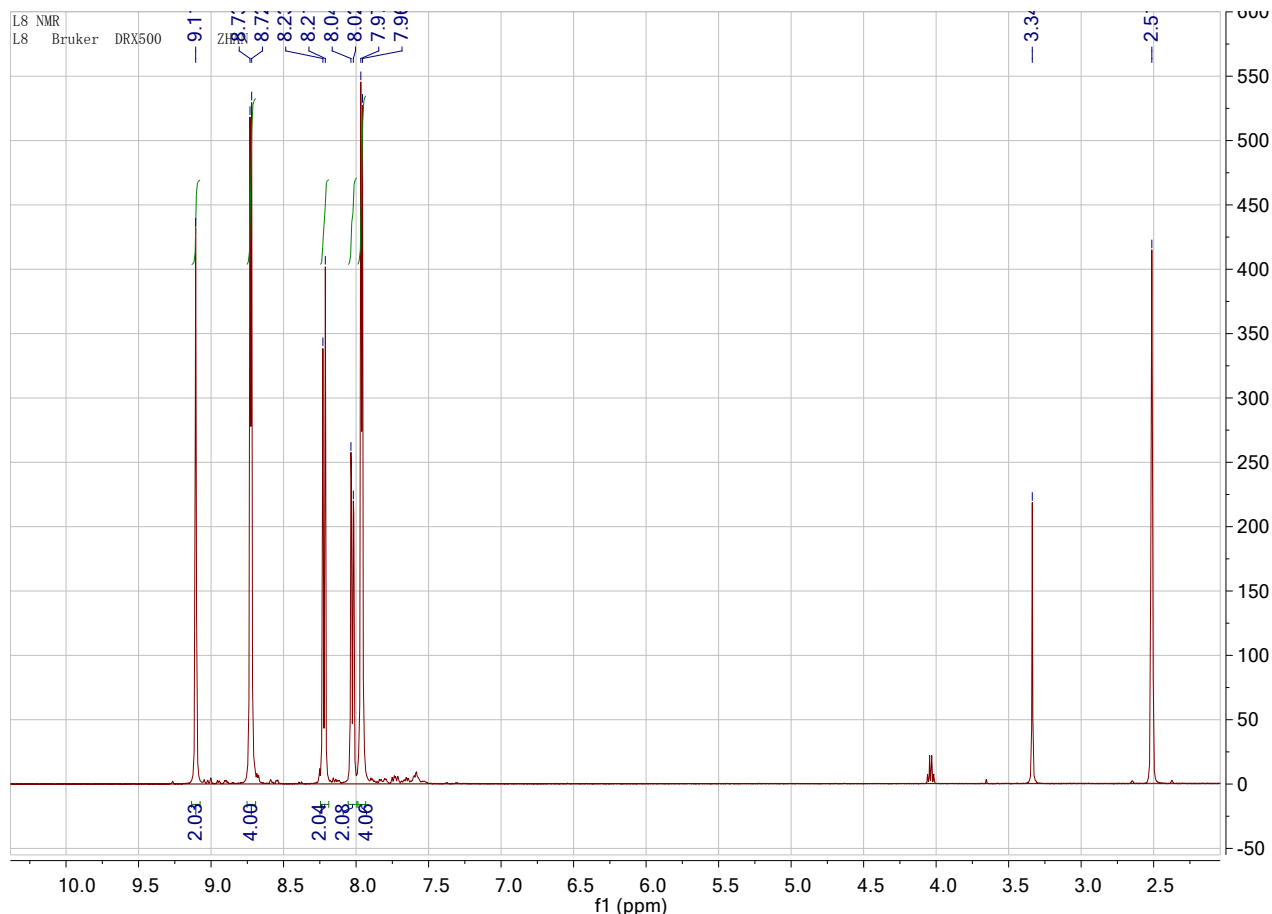


Fig. S2. ^1H NMR (DMSO- d_6 , 500 MHz) spectrum of DPDBT.

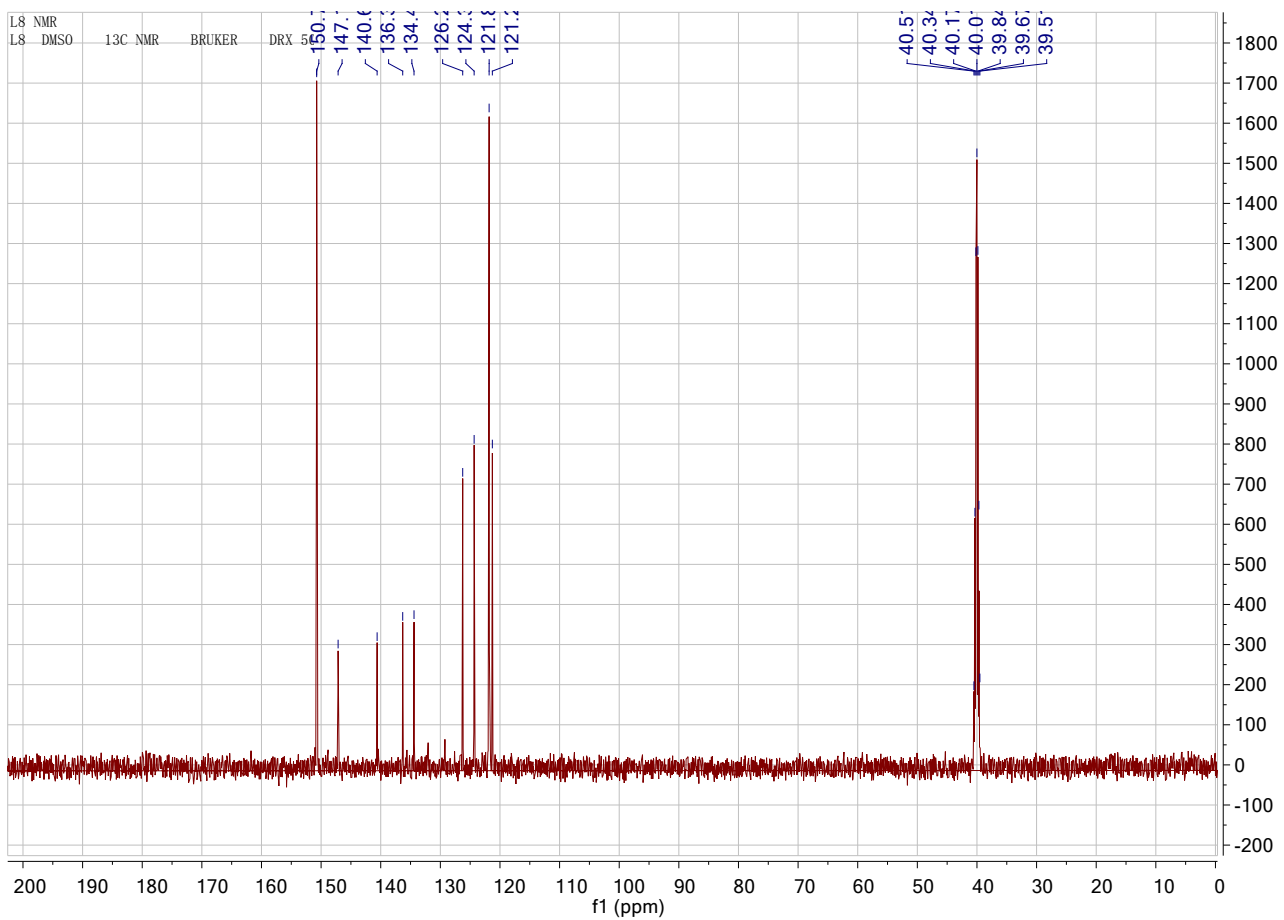


Fig. S3. ^{13}C NMR (DMSO- d_6 , 125 MHz) spectrum of DPDBT.

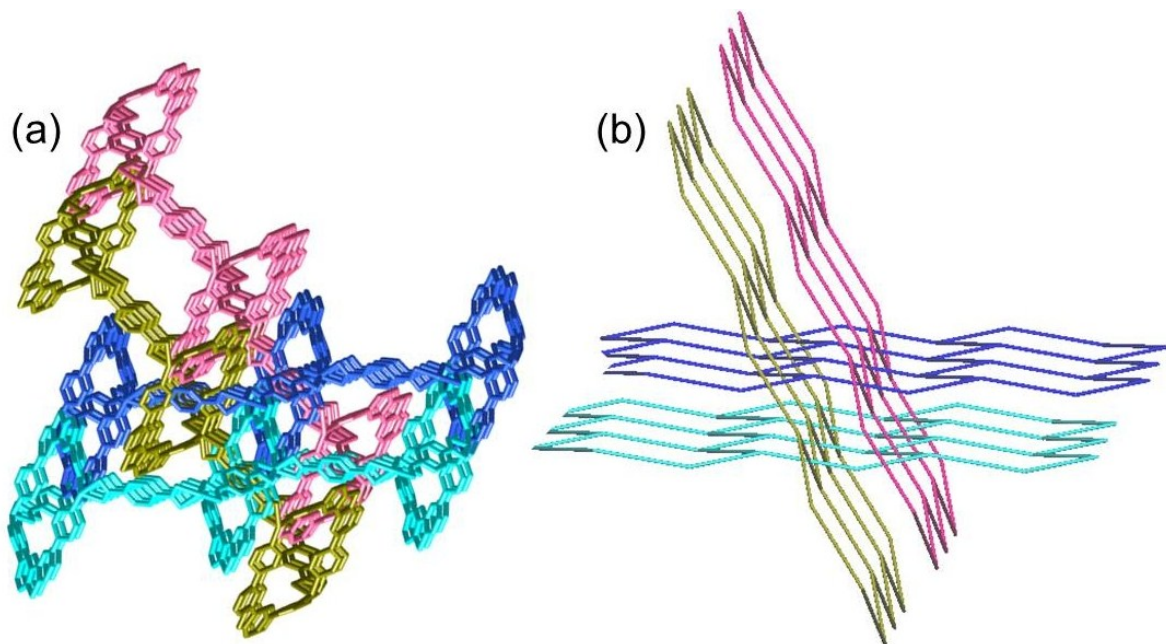


Fig. S4. (a) A view of the packing drawing of **1** along the direction parallel to the two sets of networks. (b) Simplified networks (6, 3) nets with **hcb** topology of **1**.

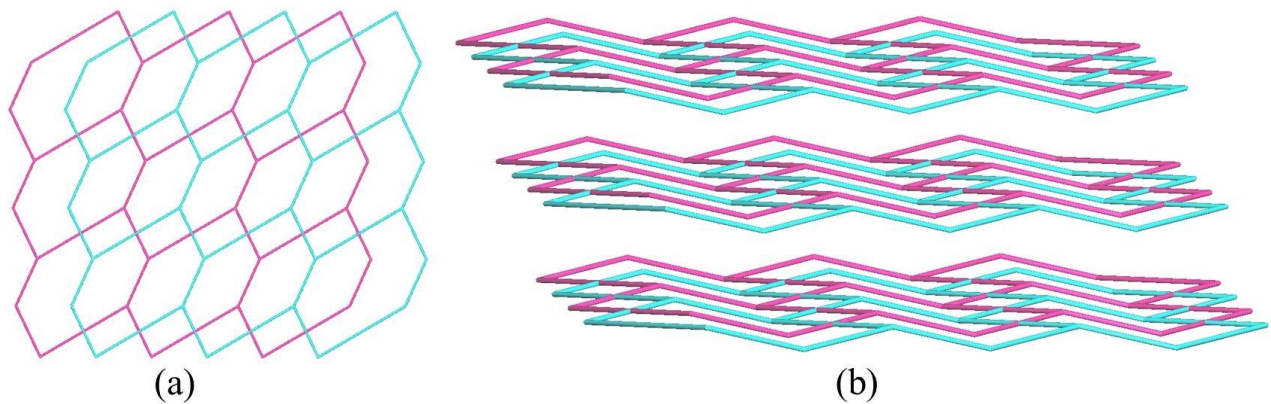


Fig. S5. (a) Simplified 2-fold interpenetrating 2D hcb network. (b) Packing drawing of the (6, 3) nets with **hcb** topology of **2**.

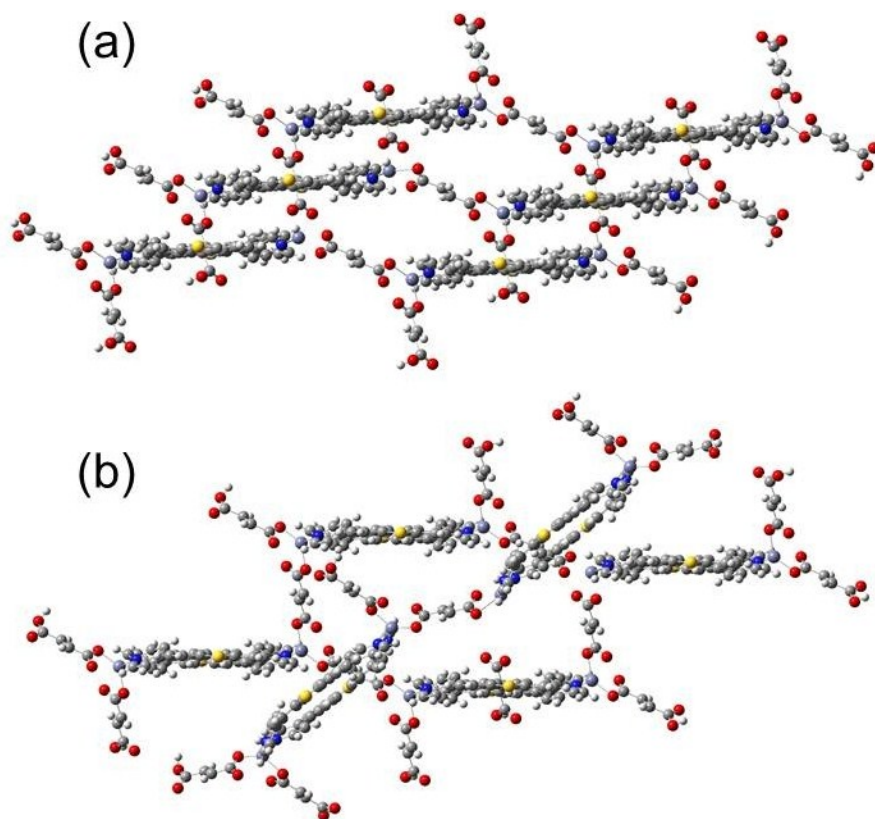


Fig. S6. (a) Parallel interlocking mode of complex **2**. (b) Inclined interlocking mode of complex **2**.

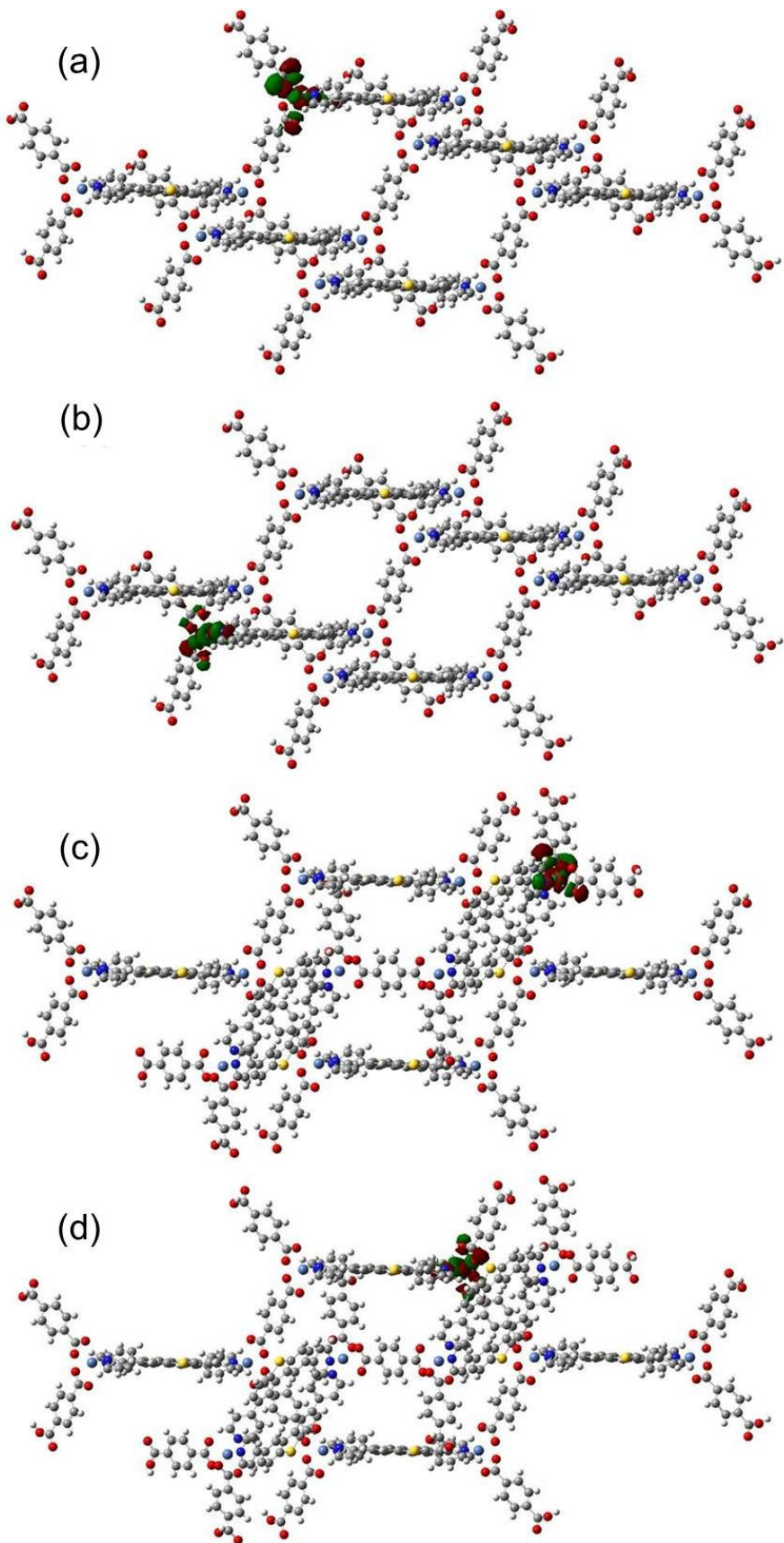


Fig. S7. Frontier molecular orbitals of networks 1: HOMO (a) and LUMO (b) with simulative parallel interlocking mode, HOMO (c) and LUMO (d) with inclined interlocking mode.

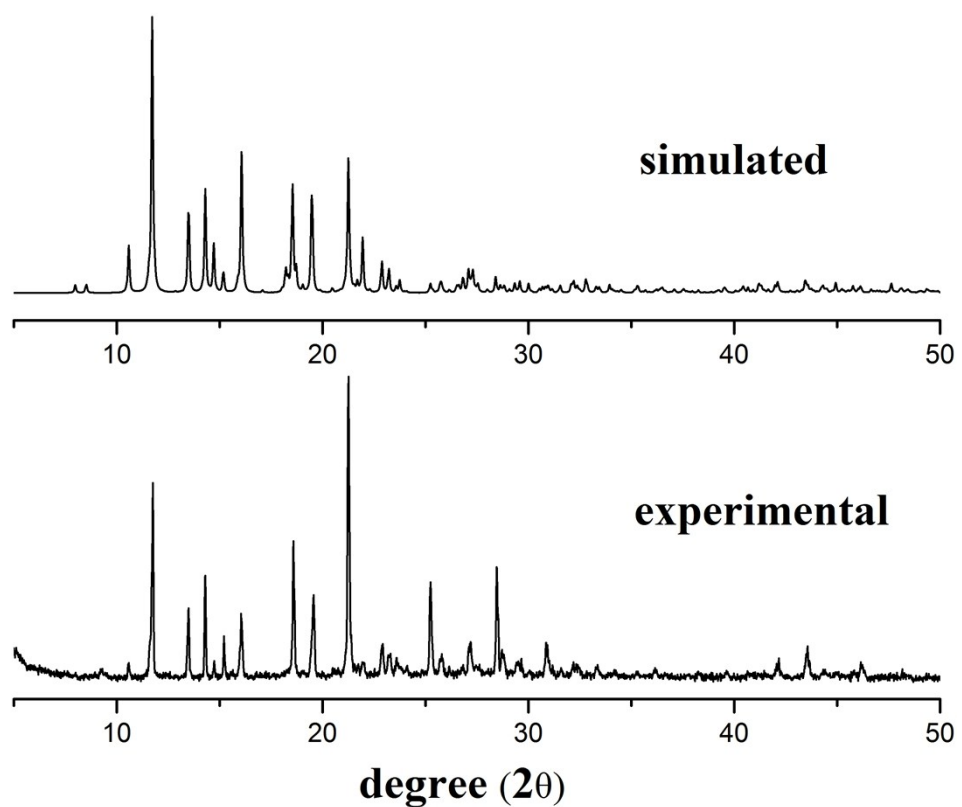


Fig. S8. Simulated and experimental PXRD plots of complex **1**.

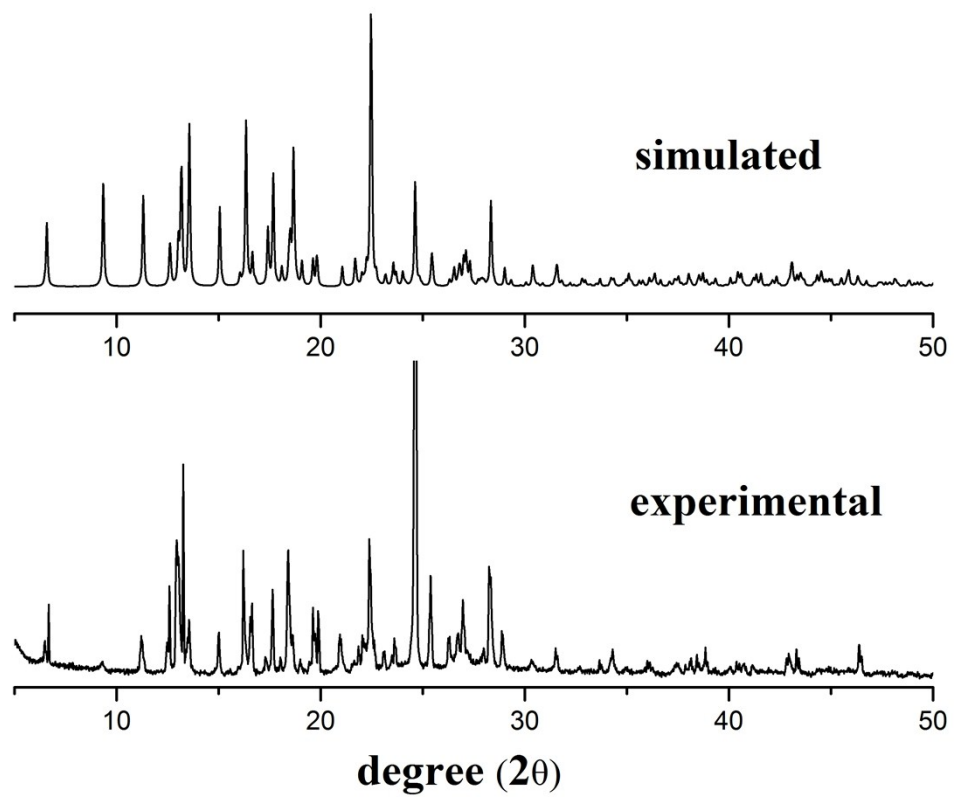


Fig. S9. Simulated and experimental PXRD plots of complex **2**.

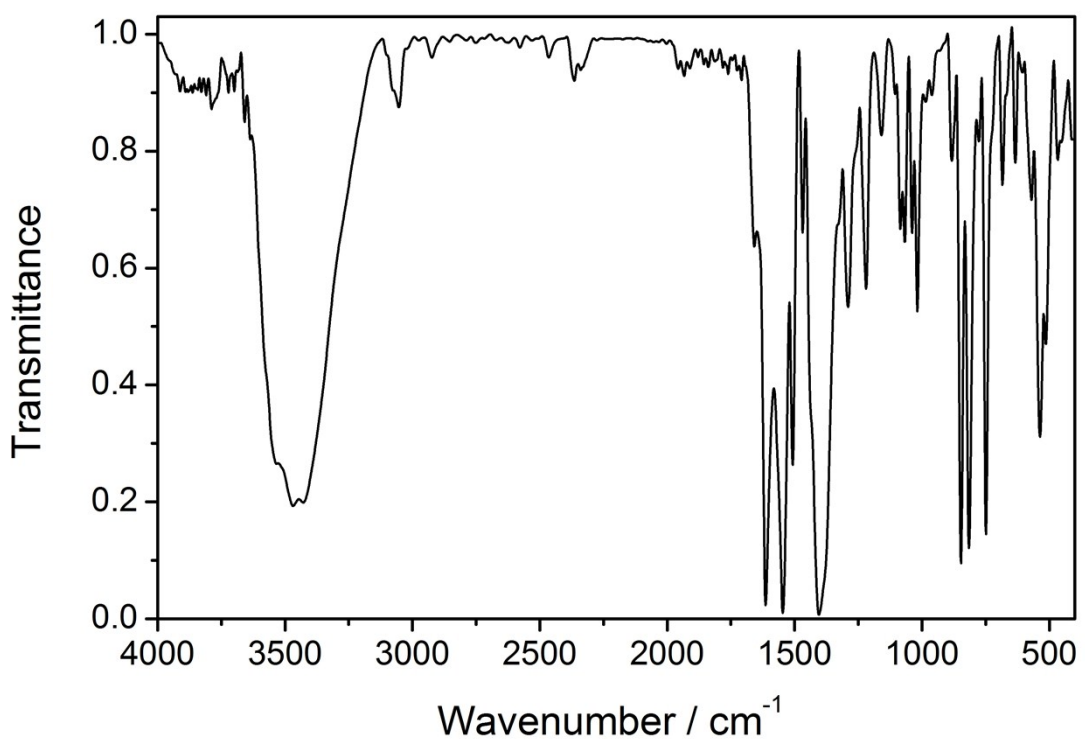


Fig. S10. IR spectrum of **1** at room temperature.

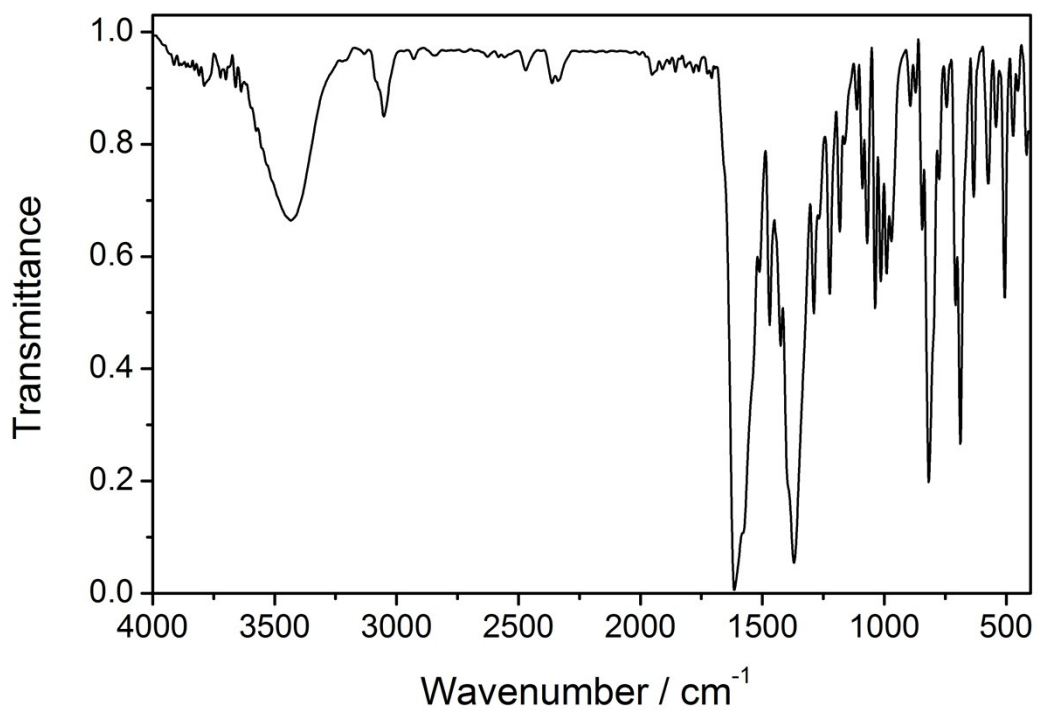


Fig. S11. IR spectrum of **2** at room temperature.